J Wood Sci (2014) 60:194–200
DOI 10.1007/s10086-014-1390-6

ORIGINAL ARTICLE

Effect of pore conformation on dielectric anisotropy of oven-dry wood evaluated using terahertz time-domain spectroscopy and eigenvalue problems for two-dimensional photonic crystals

Soichi Tanaka · Keiichiro Shiraga · Yuichi Ogawa · Yoshihisa Fujii · Shogo Okumura

Received: 28 October 2013 / Accepted: 25 December 2013 / Published online: 31 January 2014

Abstract To clarify the effect of pore conformation on the dielectric anisotropy of wood, the relative permittivity along the longitudinal and tangential axes of flat-sawn oven-dry specimens of 12 different wood species was measured using terahertz time-domain transmission spectroscopy and compared with the values calculated using the eigenvalue problem for two-dimensional photonic crystals. The measured dielectric anisotropy, which is the ratio of the relative permittivity along longitudinal axis to that along the tangential axis, was well explained by the calculated value. It was concluded that the ratio of tangential to radial widths of wood pores affects the relative permittivity along the tangential axis, and that the dielectric anisotropy decreased with an increase in the ratio. This discussion can also be applied to the relative permittivity in frequencies below 0.15 THz. These findings show promise as a new method for evaluating the porous structure of wood.

Keywords Oven-dry wood · Pore conformation · Dielectric anisotropy · THz-TDS · 2D photonic crystals

Introduction

Wood is a natural material and imposes less environmental loading than other materials such as plastics, ceramics, and metals. However, to facilitate the usage of wood in industry (such as structural members in furniture, instruments, and buildings), it is necessary to correctly evaluate fluctuating physical properties, which include its density, moisture content, and grain direction [1]. Grain direction is especially important because cross-grain cut boards and poles have inferior strength, and it has been reported that the strength of members parallel to grain is about 20 times larger than those perpendicular to grain [2]. Thus, the nondestructive evaluation (NDE) of wood grain direction is an important consideration.

The depolarization technique that uses microwaves [3–8], millimeter waves [9], and terahertz waves [10] has attracted notice as an NDE technique for wood grain direction detection because it is contact free, noninvasive, and safe as well as nondestructive. This technique is based on the phenomenon that wood depolarizes free electromagnetic waves. This wave depolarization is caused by the dielectric anisotropy of wood, which is the difference in the complex permittivities measured along longitudinal and transverse axes.

To date, numerous researchers have studied the cause of dielectric anisotropy in wood [11–27]. For example, Norimoto and Yamada [20] regarded wood as a mixture of pores and wood substance, and proposed that its dielectric anisotropy is caused by the alignment of pores and/or the dielectric anisotropy of wood substance. Tanaka et al. [23] reported that the dielectric anisotropy of oven- and air-dry

Part of this report was presented at the 38th International Conference on Infrared, Millimeter, and Terahertz Waves, Mainz, Germany September 2013.

S. Tanaka (✉)
Materials Research Institute for Sustainable Development, National Institute of Advanced Industrial Science and Technology, Nagoya 463-8560, Japan
e-mail: sch-tanaka@aist.go.jp

K. Shiraga · Y. Ogawa · Y. Fujii
Graduate School of Agriculture, Kyoto University, Kyoto 606-8502, Japan

S. Okumura
Formerly Graduate School of Agriculture, Kyoto University, Kyoto 606-8502, Japan

wood was primarily caused by the pore alignment and depended on density for a millimeter wave of 0.1 THz. Inagaki et al. [11] and Todoruk et al. [24, 25] stated that pore alignment was the major cause of dielectric anisotropy in the frequency range of 0.1–0.6 THz. However, the dielectric mixture models they used [28–33] cannot explain the relationship of the conformation of pores to the dielectric anisotropy, so alternative theoretical approaches have been sought.

The method of solving the eigenvalue problem for photonic crystals has been studied primarily to find the photonic band gap [34], which is the frequency range where electromagnetic waves are extraordinarily absorbed by photonic crystals. Fujimura [35] reported on the dielectric anisotropy of a two-dimensional (2D) photonic crystal whose structure is periodic in two axes. Since this structure is quite similar to the porous structure of wood [36–40], the above-mentioned solution method should be useful for evaluating the pore conformation of wood.

This study was performed to clarify the effect of pore conformation on the dielectric anisotropy of wood. The relative permittivity along the longitudinal and tangential axes of oven-dry flat-sawn specimens prepared from 12 different wood species was measured at a frequency of 0.15 THz using a transmission measurement system for terahertz time-domain spectroscopy (THz-TDS). Additionally, the relative permittivity was calculated by solving the eigenvalue problems for wood specimens by regarding them as 2D photonic crystals. Ultimately, the dielectric anisotropy of wood was obtained from the measured and calculated relative permittivities. The relations of two kinds of anisotropy to wood density were compared and analyzed based on the pore arrangement observed using a scanning electron microscope (SEM).

Theory

In general, wood is periodic along its radial and tangential axes [36–40] and uniform along its longitudinal axis. This structure is similar to that of a 2D photonic crystal, in which the behavior of an electromagnetic wave is theoretically analyzed by transforming Maxwell's equations to the eigenvalue equation [34, 35].

Figure 1 shows a transverse section of wood regarded as a 2D photonic crystal. In this figure, rectangular virtual unit cells, which are composed of pores (air) and wood substance [23] with relative permittivities of ε'_0 (=1) and ε'_{WS}, respectively, are arranged periodically along the elementary lattice vectors, $\boldsymbol{a}_1$ and $\boldsymbol{a}_2$. The relative permittivity, $\varepsilon'(\boldsymbol{x})$, along an arbitrary vector, $\boldsymbol{x}$, perpendicular to the longitudinal axis is determined by the radial width, a, of a virtual unit cell, the dimensional ratio, r, of its tangential to

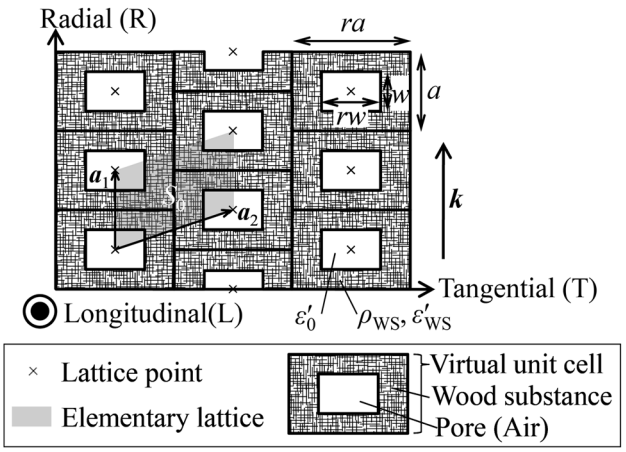

Fig. 1 Transverse section of wood regarded as a 2D photonic crystal. $\boldsymbol{k}$ represents the wave vector of an electromagnetic wave (parallel to the radial axis), ρ_{WS} the density of wood substance (=1.5 g/cm^3), ε'_0 (=1) and ε'_{WS} relative permittivities of pore (filled with air) and wood substance, respectively, w the width of a pore along the radial axis, respectively, and r is the ratio of tangential to radial widths of a pore. The rectangular virtual unit cell has a radial width of a, which is related to w, ρ_{WS}, and wood oven-dry density, ρ_0, as $a = w\sqrt{\rho_{WS}/\rho_0}$, and defines elementary lattice vectors $\boldsymbol{a}_1$ and $\boldsymbol{a}_2$. S_0 is an area of an elementary lattice

radial widths of a pore, the relative permittivity of wood substance, ε'_{WS}, and the volume fractions of the pore and wood substance, $(\rho_{WS} - \rho_0)/\rho_{WS}$ and ρ_0/ρ_{WS} [23], respectively, where ρ_0 and ρ_{WS} are the densities of oven-dry wood and wood substance, respectively. The relative permittivity function can be written as.

$$\varepsilon'(\boldsymbol{x} + \boldsymbol{a}_i) = \varepsilon'(\boldsymbol{x}) \tag{1}$$

where $\boldsymbol{a}_i$ represents the elementary lattice vectors, $\boldsymbol{a}_1$ and $\boldsymbol{a}_2$ (Fig. 1).

When Eq. (1) holds, and an electromagnetic wave transmits along the radial axis, Maxwell's equations can be transformed to the following eigenvalue equations for electric fields parallel to the longitudinal and tangential axes [34, 35].

$$\sum_{\boldsymbol{G}'} \kappa(\boldsymbol{G} - \boldsymbol{G}')|\boldsymbol{k} + \boldsymbol{G}||\boldsymbol{k} + \boldsymbol{G}'|\xi_{\boldsymbol{G}'} = k_0^2 \xi_{\boldsymbol{G}} \tag{2}$$

$$\sum_{\boldsymbol{G}'} \kappa(\boldsymbol{G} - \boldsymbol{G}')(\boldsymbol{k} + \boldsymbol{G}) \cdot (\boldsymbol{k} + \boldsymbol{G}')\varphi_{\boldsymbol{G}'} = k_0^2 \varphi_{\boldsymbol{G}} \tag{3}$$

where k_0 and $\boldsymbol{k}$ represent the scalar wave number in a vacuum and the wave vector in wood (Fig. 1) of an electromagnetic wave, respectively, $\boldsymbol{G}$ and $\boldsymbol{G}'$ are arbitrary reciprocal lattice vectors, $\xi_{\boldsymbol{G}}$, $\xi_{\boldsymbol{G}'}$, $\varphi_{\boldsymbol{G}}$, and $\varphi_{\boldsymbol{G}'}$ are eigenfunctions, and $\kappa(\boldsymbol{G} - \boldsymbol{G}')$ is expressed as follows:

$$\kappa(\boldsymbol{G} - \boldsymbol{G}') = \frac{1}{S_0} \int_{S_0} \frac{1}{\varepsilon'(\boldsymbol{x})} \exp\{-i(\boldsymbol{G} - \boldsymbol{G}') \cdot \boldsymbol{x}\} d\boldsymbol{x} \tag{4}$$

where S_0 is an area of an elementary lattice (Fig. 1).

The relative permittivity of wood can be calculated using the following steps:

1. $\varepsilon'(\boldsymbol{x})$ is determined by ρ_0, ρ_{WS}, ε'_{WS}, r, and a (Fig. 1) and substituted in Eq. (4) to obtain $\kappa(\boldsymbol{G} - \boldsymbol{G}')$.
2. $\boldsymbol{k}$ and $\kappa(\boldsymbol{G} - \boldsymbol{G}')$ are substituted in Eqs. (2) and (3) to obtain eigenvalues k_0^2 for electric fields parallel to the longitudinal and tangential axes, respectively.
3. The relative permittivities along the longitudinal and tangential axes, ε'_L and ε'_T, are calculated using the relations of k (= $|\boldsymbol{k}|$) to k_0 obtained in Step 2 for the corresponding axes and the following equation:

$$\varepsilon' = \left(\frac{k}{k_0}\right)^2 \tag{5}$$

In Eq. (5), the effective medium approximation is assumed [35], i.e., $ka/2\pi$ is less than 1/10 [32].

Experimental

Sample preparation and SEM observation

Flat-sawn specimens, 25 mm square and 3 mm thick, were cut from softwoods: hinoki (*Chamaecyparis obtusa*), sugi (*Cryptomeria japonica*), and akamatsu (*Pinus densiflora*); ring-porous hardwoods: kiri (*Paulownia tomentosa*), kuri (*Castanea crenata*), and keyaki (*Zelkova serrata*); diffuse-porous hardwoods: kusunoki (*Cinnamomum camphora*), tochinoki (*Aesculus turbinata*), buna (*Fagus crenata*), isunoki (*Distylium racemosum*), and ekki (*Lophira alata*); and radial-porous hardwood: shirakashi (*Quercus myrsinaefolia*). Five specimens were prepared for each species. All specimens were dried to a constant weight at 105 °C.

Specimens were also prepared from the blocks adjacent to the flat-sawn specimens for each species. Their transverse sections were cut by a microtome, conditioned to 0 % moisture content, covered with gold using the spatter coating process, and then observed using a scanning electron microscope (JSM-5600ED, JEOL Ltd.).

THz-TDS transmission measurement

The terahertz technique, which has been the subject of extensive research recently, makes it possible to detect the terahertz waves that penetrate through and reflect from wood specimens [10, 11, 24, 25, 41–43]. Figure 2a shows the experimental setup of the THz-TDS transmission measurement system (TAS7500SP, Advantest Co.). In operation, a THz emitter was irradiated by a femtosecond laser pulse to obtain a THz pulse. The THz pulse was then radiated to a specimen via a set of off-axis parabolic mirrors. The transmitted pulse was focused by another set of

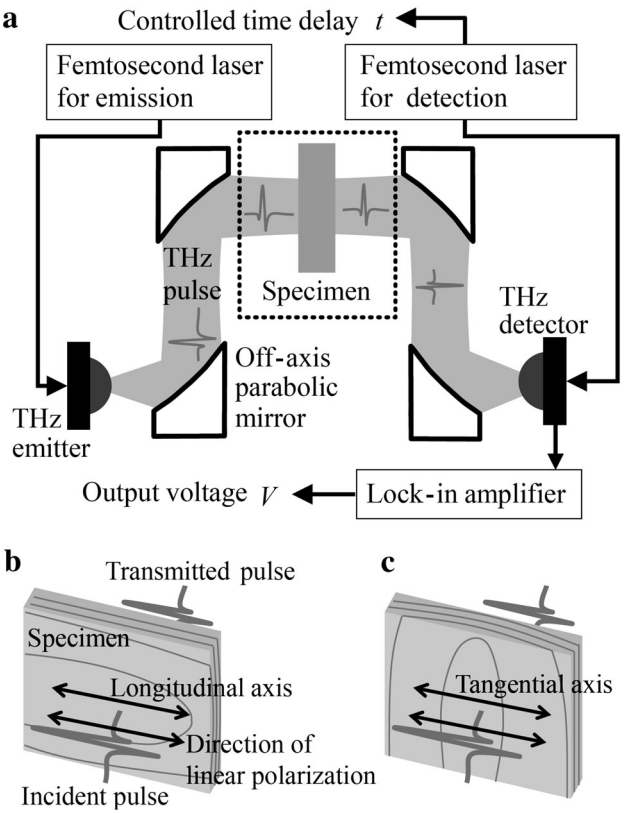

Fig. 2 Experimental setup for terahertz transmission time-domain spectroscopy. A specimen is set in the region surrounded by the *dotted line* in **a** so that its **b** longitudinal or **c** tangential axis is parallel to the direction of polarization of the terahertz pulse

off-set parabolic mirrors with a diameter of 25.4 mm and a focal length of 101.6 mm on a THz detector, in which the pulse component was synchronized with another femtosecond laser pulse, of which the time delay, t (ps), was changed stepwise at constant intervals (2 fs), detected, and processed into a voltage, V (mV) in a lock-in amplifier. The voltage V for each time delay t was measured 4096 times and averaged to obtain the waveform $V(t)$.

The phase θ (rad) and amplitude A (mV) at a frequency of 0.15 THz were obtained through Fourier transformation of the waveform $V(t)$. The relative permittivity of the specimen, ε', was obtained using the following equation:

$$\varepsilon' = n^2 - \kappa^2 \tag{6}$$

where n and κ are the refractive index and extinction coefficient, respectively, and formulated as follows:

$$n = 1 + \frac{(\theta - \theta_0)}{k_0 d} \tag{7}$$

$$\kappa = -\frac{1}{k_0 d} \ln\left\{\frac{(1+n)^2}{4n}\frac{A}{A_0}\right\} \tag{8}$$

where θ_0 and A_0 represent the phase and amplitude without a specimen, respectively, and d represents the specimen

thickness (=3 mm). k_0 is related to the wavelength in a vacuum, λ_0 (=2 mm at a frequency of 0.15 THz), as $k_0 = 2\pi/\lambda_0$.

In the region surrounded by the dotted line in Fig. 2a, the beam component of the THz pulse at 0.15 THz was approximately collimated and found to have a width of about 21.4 mm. The specimens were set on the measurement system so that the direction of linear polarization of the THz pulse was parallel to the longitudinal and tangential axes of wood to obtain the relative permittivity along the corresponding axes, ε'_L and ε'_T, respectively (Fig. 2b, c).

Results and discussion

Relation of relative permittivity to wood density

The relations of relative permittivity along the longitudinal and tangential axes, ε'_L and ε'_T, to the oven-dry density, ρ_0, for all the wood specimens are shown by plots in Fig. 3a. Here, it can be seen that ε'_L is consistently larger than ε'_T. This indicates that wood is a dielectric anisotropic material. Furthermore, ε'_L and ε'_T increased with density, ρ_0, and there was little effect of wood species. This corresponds well with the results of previous studies [11, 23] and indicates that the density dependence of the dielectric permittivity can be explained by a simple dielectric mixture composed of air and wood substance [11, 12, 20, 23, 24]. It was also indicated, from the linear relation of ε'_L to ρ_0, that the relative permittivity along the longitudinal axis of wood can be described as a simple rule of mixture, $\varepsilon'_L = \varepsilon'_0 + (\varepsilon'_{WS} - \varepsilon'_0)\rho_0/\rho_{WS}$ [23], where the relative permittivities of air and wood substance are ε'_0 (=1) and ε'_{WS}, respectively, and where ρ_{WS} is the oven-dry density of wood substance (=1.5 g/cm^3 [44]). The regression line of this equation, shown by a gray line in Fig. 3a, fitted well with the plots of ε'_L ($\varepsilon'_L = 1 + 1.63\rho_0$, $R^2 = 0.991$), and the relative permittivity of wood substance was estimated as $\varepsilon'_{WS} = 3.45$. This agrees with the results obtained using a 100 GHz-millimeter wave [23].

Numerical calculation of relative permittivity

The relative permittivity along the longitudinal and tangential axes, ε'_L and ε'_T, were numerically calculated using the process described in Theory with the parameters $\rho_0 = 1$–1.5 g/cm^3, $\rho_{WS} = 1.5$ g/cm^3, $\varepsilon'_{WS} = 3.45$, $r = 1/2$, 1, 2, and 8, and $ka/2\pi = 1/1000$–$1/10$. In the process, Eq. (4) was calculated in a discrete form using $\varepsilon'(\boldsymbol{x})$ of a 121×121 matrix, in which the elements are required to be the real number to deduce Eqs. (2)–(4) from Maxwell's equations. The dielectric loss of wood, which was estimated using $\varepsilon' = 2n\kappa$ and Eqs. (7) and (8), can probably be ignored because the ratio of the dielectric loss to the relative permittivity was at most 0.15 in the measurement. The relative permittivity was constant over the range from 1/1000 to 1/10 of $ka/2\pi$ and was reported to be constant when $ka/2\pi$ was less than 1/1000 [35]. Thus, this confirms that the effective medium approximation is valid for $ka/2\pi$ less than 1/10 [32]. In general, the dimension of the transverse section of the wood cell lumens is about less than 200 μm. Accordingly, the calculated relative permittivity is expected to be valid in wavelengths above 2 mm, or frequencies below 0.15 THz.

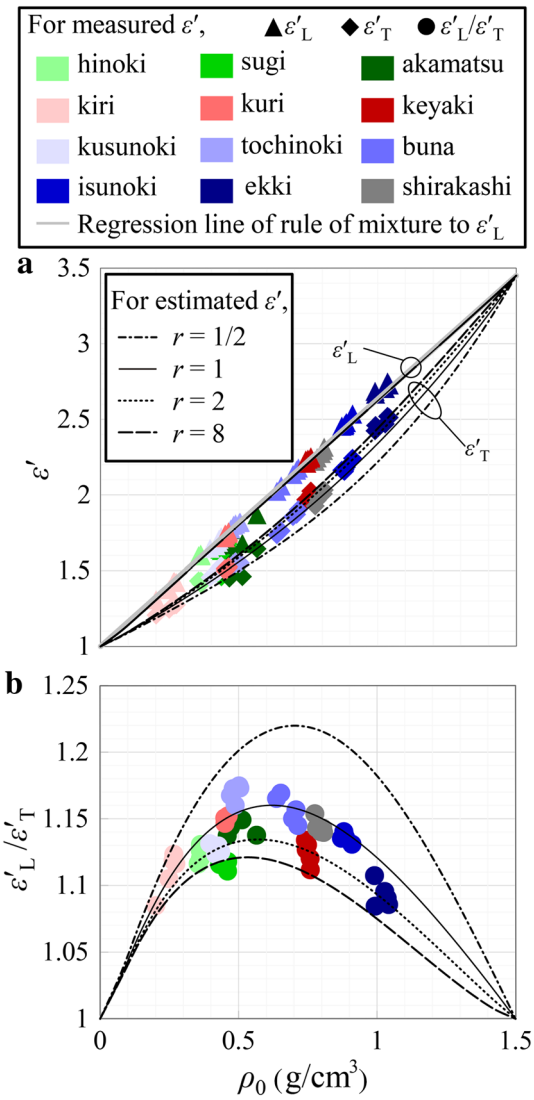

Fig. 3 Relations of **a** relative permittivity and **b** dielectric anisotropy along the longitudinal and tangential axes, ε'_L and ε'_T, to the density, ρ_0, of oven-dry wood at a frequency of 0.15 THz. The *gray line* in **a** represents the regression line ($\varepsilon'_L = 1 + 1.63\rho_0$, $R^2 = 0.991$) based on the rule of mixture for the relative permittivity along the longitudinal axis [23]

Comparison of relations of relative permittivity to wood density with calculated ones

The calculated relations of ε'_L and ε'_T to ρ_0 are shown by black lines in Fig. 3a. The calculated lines for ε'_L coincided well with each other, and also matched the regression line based on the rule of mixture, while the lines for ε'_T shifted slightly upwards with an increase in r. This indicates that the ratio, r, of the tangential to radial widths of a pore (Fig. 1), affects the relative permittivity along the tangential axis, but does not affect the relative permittivity along the longitudinal axis. The calculated lines fitted well with the measured values of ε'_L and ε'_T. This indicates that the relative permittivity of wood is explained by the eigenvalue problem for 2D photonic crystals.

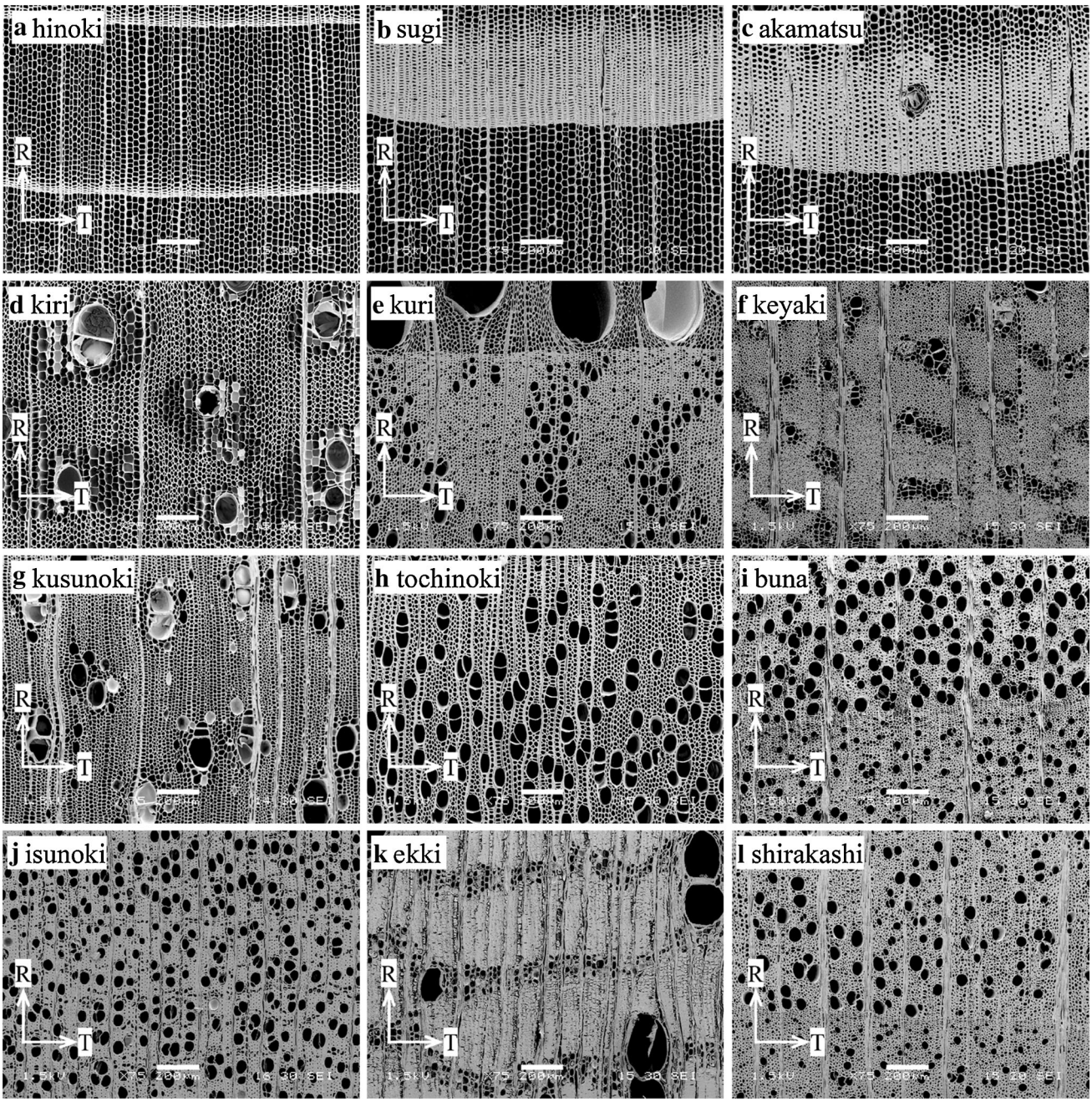

Fig. 4 SEM photographs of transverse sections of **a** hinoki, **b** sugi, **c** akamatsu, **d** kiri, **e** kuri, **f** keyaki, T and R axis labels show tangential and radial directions, respectively. *Scale bars* 200 μm, **g** kusunoki, **h** tochinoki, **i** buna, **j** isunoki, **k** ekki, and **l** shirakashi

Comparison of measured and calculated relations of dielectric anisotropy to wood density

The relations of the dielectric anisotropy, $\varepsilon'_L/\varepsilon'_T$, to ρ_0 for the measured and calculated permittivities are shown in Fig. 3b. SEM photographs of the transverse sections for all the examined wood species are shown in Fig. 4. The dielectric anisotropy, $\varepsilon'_L/\varepsilon'_T$, decreased with an increase in r and the majority of the measured values were distributed in the area surrounded by the calculated lines for $r = 1/2$ and 8 (Fig. 3b). This probably results from the effect of r on the relative permittivity along the tangential axis (Fig. 3a).

The following discussion on the relation of the dielectric anisotropy at 0.15 THz (Fig. 3b) to the porous structure of wood (Fig. 4) is limited to the pores with sizes less than about 200 μm, because $ka/2\pi < 1/10$ was assumed in the theory [32]. For softwood species (hinoki, sugi, and akamatsu), the plots of $\varepsilon'_L/\varepsilon'_T$ were in the range of $r \geq 1$. This is because the transverse section of their tracheids is rectangular and elongated along the tangential axis in latewood while it is almost square in earlywood (Fig. 4a–c). For kusunoki, ekki, and keyaki, the plots were around the line for $r = 2$. This is because the tangential widths of their fibers are larger than the radial ones for kusunoki and ekki (Fig. 4g, k) and the tangential widths of the aggregation of vessels in the latewood of keyaki are larger than the radial ones (Fig. 4f). For kuri, buna, isunoki, and shirakashi, the plots were roughly along the line for $r = 1$. This results from the fact that the tangential and radial widths of vessels and fibers are almost the same for these species (Fig. 4e, i, j, and l). For kiri and tochinoki, the plots of $\varepsilon'_L/\varepsilon'_T$ were in the range of $r \leq 1$, which is due to the radially elongated rectangles of the transverse sections of fibers and vessels (Fig. 4d, h). These findings show that the wood dielectric anisotropy is explained by the eigenvalue problem for 2D photonic crystals, and that the dielectric anisotropy undoubtedly depends on the ratio of tangential to radial widths of the wood cells.

Conclusion

To clarify the effect of pore conformation on the wood dielectric anisotropy, the relative permittivity of flat-sawn specimens of 12 wood species along their longitudinal and tangential axes was measured using the transmission measurement system for THz-TDS at a frequency of 0.15 THz. The relative permittivity was also calculated by solving eigenvalue problems for two-dimensional photonic crystals composed of wood substance and pores with the ratio of tangential to radial widths, r. The measured relative permittivity along the longitudinal axis showed a linear relation to wood density, and the relative permittivity of wood substance, ε'_{WS}, was estimated to be 3.45 by fitting the line based on a rule of mixture. The dielectric anisotropy, which is the ratio of relative permittivity along the longitudinal axis to that along the tangential axis, was well explained by the calculated permittivity with the values of $\varepsilon'_{WS} = 3.45$ and $r = 1/2$, 1, 2, and 8. It was concluded that the ratio of the tangential to radial widths of pores in wood affects its relative permittivity along the tangential axis, and that the dielectric anisotropy decreased with an increase in the ratio. The relative permittivity calculated in this study can be applied to that in the frequency range below 0.15 THz if the effective medium approximation is valid. These findings show a promising new method for evaluating the porous structure of wood.

Acknowledgments The authors would like to express their gratitude to Motoki Imamura and Akiyoshi Irisawa (Advantest Corporation, Japan) for their technical support, and to Ryota Kodama (Laboratory for Complex Energy Processes, Kyoto University) for his advice regarding the application of an eigenvalue problem for 2D photonic crystals to the analysis of dielectric anisotropy of wood.

References

1. Beall FC (2000) Subsurface sensing of properties and defects in wood and wood products. Subsurf Sens Tech Appl 1:181–204
2. Forest Products Laboratory (1999) Wood handbook: wood as an engineering material. USDA Forest Service, Madison (Chapter 4)
3. Bucur V (2003) Nondestructive characterization and imaging of wood. Springer, Berlin, pp 125–179
4. James WL, Yen Y–H, King RJ (1985) A microwave method for measuring moisture content, density, and grain angle of wood. Research note FPL–0250
5. Martin P, Collet R, Barthelemy P, Roussy G (1987) Evaluation of wood characteristics: internal scanning of the material by microwaves. Wood Sci Technol 21:361–371
6. Schajer GS, Orhan FB (2005) Microwave non-destructive testing of wood and similar orthotropic materials. Subsurf Sens Technol Appl 6:293–313
7. Schajer GS, Orhan FB (2006) Measurement of wood grain angle, moisture content and density using microwaves. Holz als Roh- und Werkstoff 64:483–490
8. Shen J, Schajer G, Parker R (1994) Theory and practice in measuring wood grain angle using microwaves. IEEE Trans Instrum Meas 43:803–809
9. Tanaka S, Fujiwara Y, Fujii Y, Okumura S, Togo H, Kukutsu N, Nagatsuma T (2011) Effect of grain direction on transmittance of 100-GHz millimeter wave for hinoki (*Chamaecyparis obtusa*). J Wood Sci 57:189–194
10. Reid M, Fedosejevs R (2006) Terahertz birefringence and attenuation properties of wood and paper. Appl Opt 45:2766–2772
11. Inagaki T, Hartley ID, Tsuchikawa S, Reid M (2013) Prediction of oven-dry density of wood by time-domain terahertz spectroscopy. Holzforschung. doi:10.1515/hf-2013-0013
12. Kröner K, Pungs L (1952) Zur dielektrischen Anisotropie des Naturholzes im großen Frequenzbereich. Holzforschung 6:13–16
13. Kröner K, Pungs L (1953) Über das Verhalten des dielektrischen Verlustfaktors des Naturholzes im großen Frequenzbereich. Holzforschung 7:12–18

14. Makoviny I (1988) Zur Anisotrpie der Dielektrizitätskonstanten des Holzes in grundlegenden anatomischen Richtungen. Holztechnologie 29:210–213
15. Nakato K, Kadita S (1954) On the dielectric constant of the oven-dried wood. J Jpn For Soc 36:95–100
16. Nanassy AJ (1970) Overlapping of dielectric relaxation spectra in oven-dry yellow birch at temperatures from 20 to 100 °C. Wood Sci Technol 4:104–121
17. Nishino Y, Norimoto M (1990) Structure and anisotropy of dielectric constant in hardwood. Wood Res Tech notes Bull Wood Res Inst Kyoto Univ 26:78–90
18. Norimoto M (1976) Dielectric properties of wood. Wood Res Bull Wood Res Inst Kyoto Univ 59(60):106–152
19. Norimoto M, Hayashi S, Yamada T (1978) Anisotropy of dielectric constant in coniferous wood. Holzforschung 32:167–172
20. Norimoto M, Yamada T (1971) The dielectric properties of wood V, on the dielectric anisotropy of wood. Wood Res Bull Wood Res Inst Kyoto Univ 51:12–32
21. Peyskens E, de Pourcq M, Stevens M, Schalck J (1984) Dielectric properties of softwood species at microwave frequencies. Wood Sci Technol 18:267–280
22. Skaar C (1948) The dielectrical properties of wood at several radio frequencies. N Y State Coll For Tech Publ 69:6
23. Tanaka S, Fujiwara Y, Fujii Y, Okumura S, Togo H, Kukutsu N, Shoji M (2013) Dielectric anisotropy of oven- and air-dried wood evaluated using a free space millimeter wave. J Wood Sci 59:367–374
24. Todoruk TM, Hartley ID, Reid ME (2012) Origin of birefringence in wood at terahertz frequencies. IEEE Trans on Terahertz Sci Technol 2:123–130
25. Todoruk TM, Schneider J, Hartley ID, Reid M (2008) Birefringence of wood at terahertz frequencies. In: Proceedings of SPIE Photon North, Montreal QC, vol. 7099, 70992Q-1
26. Torgovnikov GI (1993) Dielectric properties of wood and wood-based materials. Springer, Berlin, pp 61–76
27. Uyemura T (1960) Dielectric properties of woods as the indicator of the moisture. Bull Gov For Exp Sta 119:96–172
28. Garnett JCM (1904) Colours in metal glasses and metal films. Philos Trans R Soc Lond Sect A 3:385–420
29. Lichtenecker K, Rother K (1931) Die Herleitung des logarithmischen Mischungs-gesetzes aus allegemeinen Prinzipien der stationaren Stromung. Phys Z 32:255–260
30. Zhou Q, Knighton RW (1997) Light scattering and form birefringence of parallel cylindrical arrays that represent cellular organelles of the retinal nerve fiber layer. Appl Opt 36:2273–2285
31. Reynolds JA, Hough JM (1957) Formulae for dielectric constant of mixtures. Proc Phys Soc B 70:769–775
32. Sihvola A (2000) Mixing rules with complex dielectric coefficients. Subsurf Sens Tech Appl 1:393–415
33. Zakri T, Laurent JP, Vauclin M (1998) Theoretical evidence for "Lichtenecker's mixture formulae" based on the effective medium theory. J Phys D Appl Phys 31:1589–1594
34. Sakoda K (2001) Optical properties of photonic crystals. Springer, Berlin, pp 13–21
35. Fujimura Y (2009) Theoretical study on optical characteristics of photonic crystals. Doctoral thesis of Osaka Univ
36. Fujita M, Kaneko T, Hata S, Saiki H, Harada H (1986) Periodical analysis of wood structure I: some trials by the optical Fourier transformation (in Japanese). Bull Kyoto Univ For 60:276–284
37. Fujita M, Hata H, Saiki H (1991) Periodical analysis of wood structure IV: characteristics of the power spectral pattern of wood sections and application of non-microscopic wood pictures. Mem Coll Agric Kyoto Univ 138:11–23
38. Fujita M, Saiki H, Norimoto M (1991) Anisotropic periodicity analysis on cell distribution and microfibril orientation by the various diffraction methods. In: Grant-in-aid for scientific research (category B) result report from Japan Society for the promotion of science
39. Hata S, Fujita M, Saiki H (1989) Periodical analysis of wood structure II: dimensional arrangements of rays (in Japanese). J Soc Mater Sci Jpn 38:733–739
40. Midorikawa Y, Ishida Y, Fujita M (2005) Transverse shape analysis of xylem ground tissues by Fourier transform image analysis I: trial for statistical expression of cell arrangements with fluctuation. J Wood Sci 51:201–208
41. Jackson JB, Mourou M, Labaune J, Whitaker JF, Duling IN, Williamson SL, Lavier C, Menu M, Mourou GA (2009) Terahertz pulse imaging for tree-ring analysis: a preliminary study for dendrochronology applications. Meas Sci Technol 20:075502–075511
42. Jiang L, Li C, Huang L, Zhang Z, Zhang C, Liu Y (2012) Investigation of Terahertz spectral signatures of DNA of pine wood nematode. Adv J Food Sci Technol 4:426–429
43. Koch M, Hunsche S, Schuacher P, Nuss MC, Feldmann J, Fromm J (1998) THz-imaging: a new method for density mapping of wood. Wood Sci Technol 32:421–427
44. Kollmann F (1951) Technologie des Holzes und Der Holzwerkstoffe I. Springer, Berlin, pp 331–333